AD-A174 464 THEORY OF LASER-INDUCED PHENOMENA ON CONVENTIONAL AND PHASE-CONJUGATED SU..(U) JOHNS HOPKINS UNIV BALTIMORE MD DEPT OF CHEMISTRY J T LIN ET AL. NOV 86 1/1

UNCLASSIFIED UBUFFALO/DC/86/TR-18 N00014-86-K-0043 F/G 7/4 NL

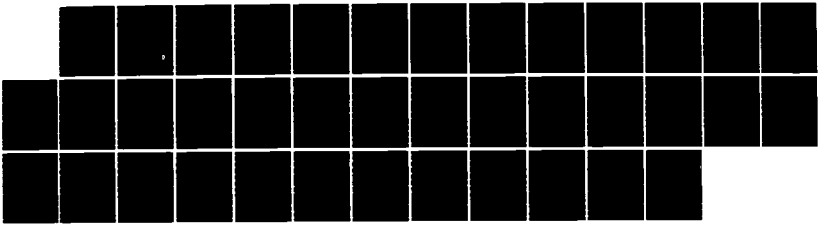

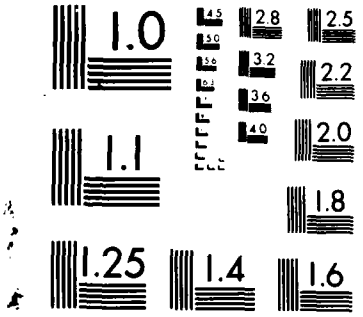

(12)

OFFICE OF NAVAL RESEARCH

Contract N00014-86-K-0043

R & T Code 413f001---01

TECHNICAL REPORT No. 18

Theory of Laser-Induced Phenomena on Conventional and Phase-Conjugated Surface

by

J. T. Lin, Xi-Yi Huang and Thomas F. George

Prepared for Publication

in

Journal of the Optical Society of America B

Departments of Chemistry and Physics
State University of New York at Buffalo
Buffalo, New York 14260

November 1986

UNCLASSIFIED

SECURITY CLASSIFICATION OF THIS PAGE

REPORT DOCUMENTATION PAGE

1a. REPORT SECURITY CLASSIFICATION Unclassified	1b. RESTRICTIVE MARKINGS
2a. SECURITY CLASSIFICATION AUTHORITY	3. DISTRIBUTION/AVAILABILITY OF REPORT Approved for public release; distribution unlimited
2b. DECLASSIFICATION/DOWNGRADING SCHEDULE	
4. PERFORMING ORGANIZATION REPORT NUMBER(S) UBUFFALO/DC/86/TR-18	5. MONITORING ORGANIZATION REPORT NUMBER(S)
6a. NAME OF PERFORMING ORGANIZATION Depts. Chemistry & Physics State University of New York 6b. OFFICE SYMBOL (If applicable)	7a. NAME OF MONITORING ORGANIZATION
6c. ADDRESS (City, State and ZIP Code) Fronczak Hall, Amherst Campus Buffalo, New York 14260	7b. ADDRESS (City, State and ZIP Code) Chemistry Program 800 N. Quincy Street Arlington, Virginia 22217
8a. NAME OF FUNDING/SPONSORING ORGANIZATION Office of Naval Research 8b. OFFICE SYMBOL (If applicable)	9. PROCUREMENT INSTRUMENT IDENTIFICATION NUMBER Contract N00014-86-K-0043
8c. ADDRESS (City, State and ZIP Code) Chemistry Program 800 N. Quincy Street Arlington, Virginia 22217	10. SOURCE OF FUNDING NOS. PROGRAM ELEMENT NO. / PROJECT NO. / TASK NO. / WORK UNIT NO.

11. TITLE
Theory of Laser-Induced Phenomena on Conventional and Phase-Conjugated Surfaces

12. PERSONAL AUTHOR(S) J. T. Lin, Xi-Yi Huang and Thomas F. George

13a. TYPE OF REPORT	13b. TIME COVERED	14. DATE OF REPORT (Yr., Mo., Day)	15. PAGE COUNT
	FROM _____ TO _____	November 1986	34

16. SUPPLEMENTARY NOTATION
Prepared for publication in the Journal of the Optical Society of America B

17. COSATI CODES			18. SUBJECT TERMS (Continue on reverse if necessary and identify by block number)
FIELD	GROUP	SUB. GR.	LASER-INDUCED SURFACE PROCESSES; RESONANCE FLUORESCENCE; CONVENTIONAL SURFACES; PERIODIC STRUCTURE; PHASE-CONJUGATED SURFACES; REFLECTIVITY

19. ABSTRACT (Continue on reverse if necessary and identify by block number)

Laser-induced processes on conventional and phase-conjugated surfaces are investigated theoretically. Resonance fluorescence of two-level atoms on smooth and rough surfaces are reviewed. The new phenomenon of a radiative dipole at a phase-conjugated surface (PCS) is examined, where the lifetime of the dipole can virtually be infinite under certain conditions. PCS originates from the interference of two laser beams incident on an absorbing layer and is discussed in terms of a phenomenological model and a hydrodynamic theory, where laser-induced periodic structure and the PCS reflectivity are analyzed. Finally, practical applications of these new phenomena occuring on PCS are discussed.

20. DISTRIBUTION/AVAILABILITY OF ABSTRACT	21. ABSTRACT SECURITY CLASSIFICATION	
UNCLASSIFIED/UNLIMITED ☒ SAME AS RPT. ☒ DTIC USERS ☐	Unclassified	
22a. NAME OF RESPONSIBLE INDIVIDUAL Dr. David L. Nelson	22b. TELEPHONE NUMBER (Include Area Code) (202) 696-4410	22c. OFFICE SYMBOL

DD FORM 1473, 83 APR EDITION OF 1 JAN 73 IS OBSOLETE.

UNCLASSIFIED

SECURITY CLASSIFICATION OF THIS PAGE

Journal of the Optical Society of America B, in press
(Feature issue on *Laser-Induced Molecular Physics at Surfaces*)

THEORY OF LASER-INDUCED PHENOMENA ON CONVENTIONAL AND PHASE-CONJUGATED SURFACES

J. T. Lin
Center of Research for Electro-Optics & Lasers
University of Central Florida
Orlando, Florida 32816

Xi-Yi Huang
Litton Guidance and Control Systems
5500 Canoga Avenue
Woodland Hills, California 91367

Thomas F. George
Departments of Chemistry and Physics & Astronomy
239 Fronczak Hall
State University of New York at Buffalo
Buffalo, New York 14260

Laser-induced processes on conventional and phase-conjugated surfaces are investigated theoretically. Resonance fluorescence of two-level atoms on smooth and rough surfaces are reviewed. The new phenomenon of a radiative dipole at a phase-conjugated surface (PCS) is examined, where the lifetime of the dipole can virtually be infinite under certain conditions. PCS originates from the interference of two laser beams incident on an absorbing layer and is discussed in terms of a phenomenological model and a hydrodynamic theory, where laser-induced periodic structure and the PCS reflectivity are analyzed. Finally, practical applications of these new phenomena occuring on PCS are discussed.

I. Introduction

During the past several years, the area of laser-induced surface chemistry (LISC) has become an established interdisciplinary pursuit among researchers in the fields of physical chemistry, material science and optics. LISC has been reviewed by several articles for various applications including microelectronics fabrication,[1-3] heterogeneous catalysis[3] and spectroscopy.[4] The fundamentals of LISC for conventional surfaces were explored in our earlier review papers,[5,6] and more recently we have studied resonance fluorescence of two-level atoms on both smooth[7,8] and rough surfaces[9] and light scattering from a metal grating.[10]

The phenomenon of phase-conjugated surfaces (PCS) has been recently explored, where both the propagation direction and the overall phase factor for an arbitrary beam of light may be precisely reversed via nonlinear optical effects.[11,12] Such effects, in general, include three-wave mixing, e.g., second-harmonic generation, parametric mixing and pockels effects, originating from the $\chi^{(2)}$ term of the susceptibility, and four-wave mixing, e.g., third-harmonic generation, Raman and Brillouin scattering, dc Kerr effects and two-photon absorption, originating from the $\chi^{(3)}$ terms of the susceptibility.

In the present paper, we shall first review LISC for conventional surfaces before presenting the new phenomena on PCS. In Section 2, we review resonance fluorescence of two-level atoms near smooth and rough surfaces. A radiative dipole near a PCS will be studied in Section 3. In Section 4, laser-induced processes at PCS will be explored in detail, where a phenomenological treatment and a hydrodynamic theory for laser-induced periodic structure and PCS reflectivity are analyzed. Applications of LISC for PCS and a summary are presented in Section 5.

II. Resonance Fluorescence of a Two-Level Atom Near a Metal Surface

The lifetime of an excited molecule has experimentally been found to vary dramatically as a function of distance from a surface.[13] It decreases or increases depending on the distance from the surface. A number of researchers have examined this effect from the viewpoint of reflected field theory, i.e., the basic calculation is concerned with the interaction between an excited molecule and its own reflected radiation field. Reflected-field theory provides generally good agreement with experiments.[7-9,13-21]

When an adatom is driven by a strong resonant, driving coherent field, it creates for the atom or molecule an environment where the probability of stimulated emission can exceed that of spontaneous emission. Under this condition, the dynamic ac Stark splitting of resonance and nutational oscillation of the emitted light intensity become important parts of the laser-driving process, such that interesting "resonance fluorescence" and other nonlinear optical phenomena can occur.[20]

We have recently derived a set of surface-dressed optical Bloch equations,[7-9,19-21] by which we can examine the dynamics and relaxation of an adatom on the surface. In these equations, we are able to evaluate the resonance fluorescence spectrum of a two-level atom near a metal surface, taking the following factors into account:

(i) The reflected electromagnetic field effects due to the presence of the interface

(ii) Collision dephasing

(iii) Surface-induced dephasing due to the reflected photons

(iv) Resonance excitation of surface plasmons

(v) Random-phase fluctuations of the laser .

Based on these studies, we have also been extending the flat-surface resonance fluorescence calculations to the rough surface case, which is modeled as a hemispheroidal protusion on a perfectly-conducting surface.[9] We would like to discuss our progress on the surface resonance fluorescence spectrum below.

A. Resonance Fluorescence at a Flat Metal Surface

Recently we have studied the resonance fluorescence spectrum of a two-level atom near a metal surface by means of a set of surface-dressed optical Bloch equations (SBE), which include the effect of surface-reflected photons, i.e., photons emitted by the laser-driven atom and reflected by the surface.[7,8] Within the rotating-wave approximation, the SBE take the form

$$\frac{d}{dt}\begin{bmatrix} \hat{S}_{21}(t) \\ \hat{W}(t) \\ \hat{S}_{12}(t) \end{bmatrix} = \begin{bmatrix} -\tilde{\gamma}_2+i\Delta & i\Omega^-(t)/2 & 0 \\ i\Omega^+(t) & -\gamma_1 & -i\Omega^-(t) \\ 0 & -i\Omega^+(t)/2 & -\tilde{\gamma}_2-i\Delta \end{bmatrix} \begin{bmatrix} \hat{S}_{21}(t) \\ \hat{W}(t) \\ \hat{S}_{12}(12) \end{bmatrix} - \begin{bmatrix} 0 \\ \gamma_1 \\ 0 \end{bmatrix} 1 \quad , \quad (1)$$

where $\hat{W} = |2><2| - |1><1|$ in the population inversion of the atom, $\hat{S}_{ij}$ is product of $\exp(i\omega_L t)$ and the transition operator $|i><j|$, $\Omega^{\pm}(t)$ is the time-dependent Rabi frequency, $\Delta = \omega_{21} - \omega_L$ is the detuning of the laser (ω_L) with respect to the two-level atom (ω_{21}), and the dephasing rate constant $\tilde{\gamma}_2$ is the sum of the radiative dephasing γ_2 and the surface-induced dephasing $\gamma_s \equiv (2/\hbar)\mathrm{Im}(f)|\mu_{12}|^2$.

To calculate γ_s, we must know the reflected field [Eq. (1)] or the complex function f(d), which can be determined by the Sommerfeld-Hertz vector procedure.[16] For the case of a laser-excited atom emitting near a metallic half-space, the imaginary part of f(d) has the form

$$\mathrm{Im}(f) = \frac{\eta}{1+\varepsilon_1^2} \frac{k_1^3}{\left(\omega^2 - \frac{\omega_p^2}{1+\varepsilon_1}\right)^2 + \frac{\delta^2\omega_p^4}{(1+\varepsilon_1)^2\omega^2}}$$

$$\times \left\{\frac{1}{\varepsilon_1}[\omega^2 - \omega_p^2)^2 + \frac{\omega_p^4\delta^2}{\omega^2} - \varepsilon_1^2\omega^4][\eta\sin D - \frac{1}{D^2}\cos D]\right.$$

$$\left. + 2\omega\delta\omega_p^2[\eta\cos D + \frac{1}{D^2}\sin D]\right\} \quad , \tag{2}$$

where $\zeta = 1$ and $\eta \equiv (1/D^3) + (1/D)$ for the case of the induced dipole oriented parallel to the surface, $\zeta = 2$ and $\eta \equiv 1/D^3$ for the perpendicular case, ε_1 is the dielectric constant for the gas medium, $k_1 = \omega\sqrt{\varepsilon_1}/c$ is the wave number, ω is the emission frequency, c is the speed of light, and $D = 2k_1 d$ is the reduced distance which is dimensionless. The Drude model[10] has been used to determine the dielectric constant of the metal medium, i.e.,

$$\varepsilon_2(\omega) = 1 - \frac{\omega_p^2}{\omega(\omega + i\delta)} \quad , \tag{3}$$

where δ is the inverse of the relaxation time and ω_p is the plasma frequency. We note that Im(f) has a resonance at $\omega_{sp} = \omega_p(1+\varepsilon_1)^{-1/2}$, which is the surface plasmon frequency of the interface, so that the reflected field given by Eq. (1) involves resonance energy transfer between the adatom and the excited surface plasmon.

In our model, the driving and reflected fields have been treated semiclassically, and we have assumed the atom-surface distance to be large ($\gtrsim$ 30 nm). The relaxation time included in the Drude model for the complex dielectric constant of the metal medium represents the dissipation of electron gas which, together with surface plasmon resonances, influences the surface reflectivity and hence the behavior of the reflected field. Here we could neglect nonradiative transfer of energy from the excited atom to the

metal. Effects of the laser bandwidth are included by means of a phase-diffusion model for the driving field. In the weak-field or large-detuning limit, the power spectrum of scattered light has two peaks: one corresponding to Rayleigh scattering at the laser frequency ω_L and the other to fluorescence at the atomic transition frequency ω_{21}. For a sufficiently strong driving laser field, the spectrum exhibits three peaks: a central one at $\omega_0 = \omega_L$ (Rayleigh component), a left one at $\omega_- = 2\omega_L - \omega_{21} - \delta$ (three-photon component) and a right one at $\omega_+ = \omega_{21} + \delta$ (fluorescence component), where δ is the ac Stark shift. Results for the peak heights H_-, H_0 and H_+ are shown in Fig. 1 for the case of a silver surface.[8] The key feature, which is a unique behavior due to the surface, is that for certain atom-surface distances H_- is larger than H_+, whereas in the pure gas-phase resonance fluorescence spectrum H_- is always less than H_+ (due to molecular collisions for positive detuning). Also, the population inversion of the adatom and the resonance fluorescence spectrum, as well as the surface-induced phase-decay constant of the adatom, show strong oscillatory behavior as a function of the adatom-surface distance.[7,8]

B. Resonance Fluorescence at a Rough Surface

For a rough surface, let us consider a surface protusion modeled by a prolate hemispheroid on top of a plane.[9,22,23] We note that this model has been shown to be identical to a full spheroid in a vacuum,[24] so that our calculations can also be used for an ellipsoidal cluster. The two-level adatom, which is located at a distance d from the top of the hemispheroid, is driven by a laser. The prolated spheroidal coordinates (ξ,η,ϕ) are used to calculate the reflected field. We define

$$\xi_1 = (a + d)/f \tag{4}$$

$$\xi_0 = a/f \tag{5}$$

and

$$f = (a^2 - b^2)^{1/2} \quad , \tag{6}$$

where a and b are the semi-major and semi-minor axes of the hemispheroid. The reflected field at the position of the adatom (transition dipole) in the near-field approximation can be written as[22]

$$E_r = -\frac{1}{f}\sum_n{}' C_n Q_n'(\xi_1) + \frac{\mu}{4(f\xi_1)^3} \quad , \tag{7}$$

where Q_n denotes the Legendre function of the second kind and μ is the induced dipole moment. The expansion coefficient C_n depends on the laser amplitude E_0 and parameters ξ_0 and ξ_1. Based on the surface-dressed optical Bloch equations[7,8] appropriate for the excitation and dissipation of a two-level adatom near a hemispheroid, we find the surface-induced phase relaxation constant γ_s to be given by

$$\gamma_s = (2/\hbar)\mathrm{Im}(F) \quad , \tag{8}$$

where

$$F = \frac{1}{1-\Gamma}\left[\frac{(1-\epsilon)\xi_0 Q_1'(\xi_1)}{\epsilon Q_1(\xi_0) - \xi_1 Q_1'(\xi_0)} + \Gamma\right] \quad , \tag{9}$$

where ϵ is the complex dielectric constant and Γ is a somewhat complicated function of ξ_0, ξ_1 and ϵ.

A sharp resonance enhancement of the adatom-hemispheroid interaction, through the reflected field at the atomic site, occurs when the specific shape of the prolate hemispheroid corresponds to a resonant excitation of plasmons (see Fig. 2). The time oscillation of the level population

decreases as the shape of the hemispheroid approaches the plasmon resonance. We also find that the strong-field three-peak fluorescence spectrum is strongly influenced by the roughness of the surface. The resonance excitation of the plasmon in the hemispheroid remarkably enhances the adatom-surface coupling, such that the dephasing processes broaden the linewidths of the spectrum. In the small detuning case, the spectrum has a distinctive three-peak nature, where the three-photon side peak has a measurable height which is almost comparable to the fluorescence side peak. The plasmon and reflected-field broadening influence equally the three spectral peaks. In the large detuning case, the height of the three-photon peak is decreased, and the three-peak spectrum is transformed to the weak-field two-peak structure.

III. Radiative Dipole in the Presence of a Phase-Conjugated Surface

A. Phase-Conjugated Mirror Cavity

Recently, we have evaluated the lifetime variation of a dipole centered in a spherical cavity made by a phase conjugated mirror (PCM)[26] (see Fig. 3).

Following Kuhn,[27] the equation of motion of the dipole μ (assumed to be harmonically-bound charge) can be written as

$$\ddot{\mu} + \omega^2\mu = \frac{e^2}{m} E_R - b_0\dot{\mu} \quad , \tag{10}$$

where ω is the oscillation frequency in this absence of all damping, m is the effective mass of the dipole, E_R is the reflected field at the dipole position due to the presence of the PCM cavity, and b_0 is the damping constant (inverse lifetime) in the absence of the mirror. The dipole moment μ and the (complex) reflected field E_R oscillate at the same frequency, i.e.,

$$\mu = \mu_0 \, e^{-i[\omega + \Delta\omega]t} \, e^{-bt/2} \tag{11}$$

and

$$E_R = E_R^0 \, e^{-i[\omega + \Delta\omega]t} \, e^{-bt/2} \quad , \tag{12}$$

where μ_0 and E_R^0 are the amplitudes of the dipole oscillator and reflected field, respectively, and $\Delta\omega$ and b are the frequency shift and the inverse of the lifetime, respectively, in the presence of the PCM cavity. The frequency shift is found to be quite small and is thus unimportant for the purpose of discussion in the paper. Recognizing that b^2 and the magnitude of $(e^2/\mu_0 m)E_R^0$ are normally very small compared to ω^2, we then have

$$b = b_0 + \left[\frac{e^2}{2\mu_0 m\omega}\right] I_m(E_R^0) \quad . \tag{13}$$

To examine the variation of dipole lifetime, we reduce the problem to the calculation of the reflected field by the PCM at the dipole position.

By using the Hertz vector method,[28] the field near the dipole is easily found to be

$$E_r \cong 2\mu_0 k^{*3} (\eta_1 + i\eta_2)\left[\frac{1}{(k^* r_0)^3} - \frac{i}{(k^* r_0)^2}\right] \cos\theta \, e^{-i\omega^* t} \tag{14}$$

$$E_\theta \cong \mu_0 k^{*3} (\eta_1 + i\eta_2)\left[\frac{1}{(k^* r_0)^3} - \frac{i}{(k^* r_0)^2}\right] \sin\theta \, e^{-i\omega^* t} \quad , \tag{15}$$

where r_0 is the linear dimension of the dipole (normally $k^* r_0 \ll 1$), and $\eta = \eta_1 + i\eta_2$ is the complex reflectivity of the PCM mirrors where

$$\omega^* = \omega - i\frac{b}{2} = ck^* \quad , \tag{16}$$

c is velocity of light, and the definitions of E_r, E_θ, θ and r are readily shown in Fig. 3. We note that $b \ll \omega$, and taking an average with respect to

θ for the field at the dipole site, we obtain the imaginary part of the reflected field as

$$\mathrm{Im}(E_R^0) \cong \frac{3}{2}\mu_0 k^3 \left[\frac{\eta_2}{(kr_0)^3} - \frac{\eta_2}{(kr_0)^2}\right] \quad , \tag{17}$$

where k is the propagation constant, $k = \omega/c$. The normalized decay constant is

$$\bar{b} = \frac{b}{b_0} = 1 + \Delta\bar{b}$$

$$\cong 1 + \frac{9}{8} \frac{|\eta|}{1 + (\frac{\eta_2}{\eta_1})^2} \left[\frac{\eta_2/\eta_1}{(kr_0)^3} - \frac{1}{(kr_0)^2}\right] \quad , \tag{18}$$

where $|\eta| = \sqrt{\eta_1^2 + \eta_2^2}$ is the magnitude of the reflectivity, and $\bar{b}^{-1}$ is the normalized lifetime of the dipole.

Figure 4 displays typical curves for the variation of the lifetime for a dipole in a PCM cavity, as a function of η_2/η_1 with a fixed reflectivity $|\eta|$ = 1%, 2% and 3%. It is noted that due to the focusing nature of the reflected radiation wave by the PCM, the coupling between the dipole and reflected field can be very strong. In the case of the phase-shifted reflection, i.e., $\eta_2 \neq 0$, there are three cases worthy of note:

(a) There is a critical value of η_2/η_1, defined as $(\eta_2/\eta_1)_c$, when $\eta_2/\eta_1 \to (\eta_2/\eta_1)_c$ and $b \cong 0$, i.e., in this case the lifetime b^{-1} of the dipole in the PCM cavity can be infinite.

(b) In the region $\eta_2/\eta_1 > 0$, $\bar{b} > 1$, the dipole in the PCM cavity can decay faster than that in free space.

(c) For the region of $\eta_2/\eta_1 < (\eta_2/\eta_1)_c$, the dipole decay constant $\bar{b}$ can be negative, i.e., the amplitude of the dipole oscillator can be amplified, due to the pumping process in the PCM.

IV. Laser-Induced Periodic Structure (LIPS) on Phase-Conjugated Surfaces

Laser-induced periodic structure (LIPS) on conventional surfaces has been studied over the past several years,[29] where only one laser was needed for LIPS, which has been explained by the possible mechanisms: (i) formation of a surface polariton with periodic electric field acting on the surface atoms;[19,30,31] (ii) laser-induced longitudinal acoustic phonon of the substrate which forms a standing wave;[32] and (iii) small inhomogeneities or roughness of the surface layer which interact with the incident laser and forms a dipole layer.[33] In mechanism (iii) the interference between the dipole field and the refracted field in the substrate in turn leads to inhomogeneous energy absorption and thus the redistribution of the surface atoms.

In contrast to the above described LIPS on a conventional surface, where only one laser beam is needed, two laser beams are usually required for LIPS on PCS. The novel method of LIPS on PCS using the spatially nonuniform reflectivity variation, both in amplitude and phase, of laser-influenced interface systems include: (i) electron concentration changes (for metal and semiconductor surfaces); (ii) surface deformation due to laser-induced pressure (or density) variation of the surface layer; and (iii) the nonuniform thermal expansion of the absorbing layer. Surface heating and deformation by a single pulsed laser have been reported for both metal[34] and semiconductor surfaces.[35] Laser-induced profiles of absorbing dye in solution have also been proposed, where two interfering laser beams (at the same frequencies) were used for LIPS caused by the concentration modulation of the dye.[36]

In this section, we shall present a unified treatment for LIPS on PCS based upon a hydrodynamic theory. The mechanisms of LIPS and the formation

of PCS will be explored mathematically. Special cases with analytic results and the appropriate conditions for the validity of previously published results will be discussed.

A. Phase-Conjugated Surface

Phase conjugation has been conventionally recognized using stimulated scattering (Raman, Brillouin and Rayleigh) and parametric processes (four-wave mixing and two-wave mixing).[11] The novel method of phase conjugation using the nonuniform reflectivity of the absorbing layer is shown in Fig. 5, where the initially uniform reflecting surface may form a periodic structure caused by the interference of two incident beams. This process requires the nonlinear optical effects of the surface layer, e.g., nonlinear polarization $P^{NL} \propto \vec{E}\cdot\vec{E}\cdot\vec{E}$, where $\vec{E}$ is the total wave vector given by the sum of the reference (strong) wave $\vec{E}_1$ and the signal (weak) wave $\vec{E}_3$ by

$$\vec{E} = \vec{E}_1 + \vec{E}_3 = \tfrac{1}{2}(E_1 e^{i(\omega_1 t + \vec{k}_1\cdot\vec{r})} + E_3 e^{i(\omega_3 t + \vec{k}_3\cdot\vec{r})} + \text{c.c.}) \quad . \quad (19)$$

The laser-influenced reflectivity (R), which in general is time-dependent and is a complex variable with amplitude and phase modulation, may be expressed (up to the first-order expansion of the laser intensity) as

$$R = R_0 + \beta R_1 \quad , \quad (20)$$

where R_0 is the reflectivity from a conventional surface and is proportional to the total intensity, $|E_1|^2 + |E_3|^2$. β is the expansion coefficient of the interference pattern (or reflectivity modulation) formed by the incident waves, and R_1 is given by

$$R_1 = E_1 E_3^* e^{i\Delta\vec{k}\cdot\vec{r}} + \text{c.c.} \quad , \quad (21)$$

where we have assumed the degenerate case, $\omega_1 = \omega_3$, and have used the rotating-wave approximation (RWA). $\Delta\vec{k}$ is the phase mismatching vector defined by $\Delta\vec{k} = \vec{k}_1 - \vec{k}_3$. For the one-dimensional and degenerate ($k_1 = k_3 = k$) case $|\Delta\vec{k}\cdot\vec{r}| = 2kz\sin(\theta/2)$, such that the interference pattern is governed by the angle (θ) between the incident waves. We shall show in the next section that the lifetime of the interference pattern is proportional to the inverse of $|\Delta\vec{k}\cdot\vec{r}|^2$, i.e., a small angle (in the order of few mrad) is required for a long-lived interference pattern to be observed.

The overall reflected waves defined by the laser-modulated reflectivity may now be calculated by using RWA to eliminate the irrelevant terms, whereby we obtain from Eqs. (19) and (20)

$$\vec{E}_{ref} = R(\vec{E}_1 + \vec{E}_3)$$

$$= R_0(\vec{E}_1 + \vec{E}_3) + \beta e^{-i\omega t} \sum_{m\neq n=1,3} e^{-i\vec{k}_n\cdot\vec{r}} [(E_m^* e^{-i\vec{k}_m\cdot\vec{r}})^2 E_n(-\vec{r}) + |E_m|^2 E_n^*] \quad . \tag{22}$$

Thus the total reflection field, $\vec{E}_{ref}$, consists of three parts: (i) the usual reflected fields from the the unperturbed surface, the R_0 terms; (ii) the reflected fields from the laser-perturbed surface in the usual way, i.e., from the incident $\vec{r}$ to the reflected $-\vec{r}$ direction; and (iii) the reflected fields in the phase-conjugated forms, the $E_n^*(\vec{r})$ terms. The reflectivity of the phase-conjugated surface (PCS) defined by the intensity ratio between the signal wave and its conjugation becomes

$$R_{PCS} = \beta^2|E_1|^4 = (\beta I_1)^2 \quad . \tag{23}$$

This is proportional to the square of the nonlinear coefficient of the surface layer and the intensity square of the reference wave (E_1), which is

usually much stronger than the signal wave (E_3). We note that the above obtained results involved several assumptions: (i) the pump depletion of the reference wave is ignored; (ii) steady-state reflectivity (or interference pattern) is assumed; (iii) instant energy transfer (or local heating) of the surface layer is assumed; and (iv) heat diffusion of the surface layer and attenuation of the fields are ignored. For a rigorous treatment, these assumptions will be removed in the following sections.

B. Hydrodynamic Theory for LIPS

The generation of density and temperatures fluctuations following the absorption of light is known as a stimulated thermal process, where the light-induced modulation of the refraction index of the absorbing layer can act as a phase grating in the diffration of incident light.[37] The full dynamics of a thermal grating may be described by a hydrodynamic theory which includes the thermal processes of the absorbing media and the optical nonlinear effects (or polarization) caused by laser fields. The complete set of hydrodynamic equations which couple the thermodynamic variable (density, internal energy and temperature) of the medium and the electric fields of the incident beams are given by[38]

$$\frac{\partial U}{\partial t} = \frac{nc\alpha}{4\pi} \vec{E}^2 + D\nabla^2 U - U/\tau \quad , \tag{24}$$

$$C_V \frac{\partial T}{\partial t} - K\nabla^2 T - F\frac{\partial \rho}{\partial t} = U/\tau \quad , \tag{25}$$

$$\frac{\partial^2 \rho}{\partial t^2} - B_T \nabla^2 \rho - \eta \frac{\partial}{\partial t}(\nabla^2 \rho) - F\nabla^2 T = \frac{\gamma_e}{8\pi} \nabla^2 (E^2) \quad , \tag{26}$$

$$\frac{n^2}{c^2} \frac{\partial^2 \vec{E}}{\partial t^2} - \nabla^2 \vec{E} = -\frac{4\pi}{c^2} \frac{\partial^2}{\partial t^2} \vec{P}^{NL} \quad . \tag{27}$$

Here U is the internal energy of the medium with absorption coefficient α, diffusion constant D and thermalization time τ; T and ρ describe the temperature and density fluctuation (normalized by their equilibrium values); K is the thermal conductivity and C_V is the specific heat at constant volume; F is an appropriate coupling constant and η is the effective viscosity; B_T is the bulk modulus (or thermal expansion coefficient); and γ_e is the electrostrictive constant. Equation (26) is just the usual Maxwell equation with a nonlinear polarization relating to the dielectric constant (ε), density, temperature and field amplitudes by

$$\vec{P}^{NL} = [(\frac{\partial \varepsilon}{\partial \rho})_T \rho + (\frac{\partial \varepsilon}{\partial T})_\rho T](\vec{E}/4\pi) = (\gamma_e \rho + \gamma_T T)(\vec{E}/4\pi) \quad . \tag{28}$$

Employing the slowly-varying envelop approximation (SVEA) and RWA which eliminates the irrelevant (or nonresonant) terms, we obtain a set of simplified equations for the amplitudes of the density, temperature and electric fields as

$$[\frac{\partial}{\partial t} + Dq^2 + \frac{1}{\tau}]U_1 = \frac{nc\alpha}{4\pi}(E_1 E_3^* + E_2^* E_4) \quad , \tag{29}$$

$$[\frac{\partial}{\partial t} + \frac{\gamma}{\tau_R}]T_1 - \frac{(\gamma-1)F}{B_T}\frac{\partial \rho_1}{\partial t} = \frac{F}{\tau C_v B_T} U_1 \quad , \tag{30}$$

$$[\frac{\partial^2}{\partial t^2} + \Gamma_0 \frac{\partial}{\partial t} + \frac{\omega_0^2}{\gamma}]\rho_1 + \frac{F\omega_0^2}{B_T \gamma} T_1 = \frac{\gamma_e q^2}{8\pi}(E_1 E_3^* + E_2^* E_4) \quad , \tag{31}$$

$$[\frac{\partial}{\partial z} - \frac{n}{c}\frac{\partial}{\partial t}]E_3 = -\frac{ik}{4n^2} E_1(\gamma_e \rho_1^* + \gamma_T T_1^*) \quad , \tag{32}$$

$$[\frac{\partial}{\partial z} - \frac{n}{c}\frac{\partial}{\partial t}]E_4 = \frac{ik}{4n^2} E_2(\gamma_e \rho_1 + \gamma_T T_1) \quad , \tag{33}$$

where

$$\vec{q} = \vec{k}_1 - \vec{k}_3 \quad , \quad \tau_R = C_p/Kq^2 \quad , \quad \gamma = C_p/C_V \quad , \tag{34}$$

are the k-vector and decay time of thermal grating and the specific heat ration, respectively; ω_0 and Γ_0 are the frequency and linewidth of the acoustic phonon wave given by ω_0 = wave velocity × q, $\Gamma_0 = \eta q^2$. In deriving the above equations, we have further assumed the degenerate case, $\omega_1 = \omega_3 = \omega$, $k_1 = k_3 = k = n\omega/c$ and ignored the small absorption in the thin layer, $\exp(\alpha) \cong 1$. The amplitudes of the incident ($\vec{E}_1$), reflected ($\vec{E}_2$), probing ($\vec{E}_3$) and the phase-conjugated ($\vec{E}_4$) fields, internal energy, density and the temperature are defined by

$$\vec{\psi}_j = \tfrac{1}{2}(\psi_j e^{i(\omega_j t - \vec{k}_j \vec{r})} + c.c.) \quad , \tag{35}$$

where $\psi_j = E_j, \rho_1, T_1, U_1$ with j = 1,2,3,4. Similar to that of E_3 and E_4, equations for E_1 and E_2 are not shown here. They are needed only when the pump depletion i.e., the variation of E_1 with z, is considered.

We note that within the SVEA, the thermal grating is formed in such a way that only the relevant component of the reflected wave meeting the energy and momentum conservation is strongly coupled, where the phase matching condition is met between the the probe (E_3) and the conjugated (E_4) waves through this intrinsic feature of the thermal-grating-induced acoustic wave. This feature may be clearly realized by the steady-state solutions for the coupled equations (29)-(33) which reduce to

$$\frac{dE_3}{dz} = -\beta_1 |E_1|^2 E_3 - \beta_2 E_1 E_2 E_4^* \quad , \tag{36}$$

$$\frac{dE_4}{dz} = \beta_3 |E_2|^2 E_4 + \beta_4 E_1 E_2 E_3^* \quad , \tag{37}$$

where β_j are the appropriate coupling constants, proportional to the decay time of the thermal grating defined in Eq. (34). These steady-state equations are similar to those of the degenerate four-wave mixing FWM),

where E_1 and E_2 are the pump beams and E_3 and E_4 are the signal (probe) and the conjugate beams. The first terms on the right-hand sides of the above equations describe the nonlinear refractive index changes caused by the optical Kerr effects, while the second terms account for the phase-conjugated FWM. A complete description of the dynamics of LIPS requires the numerical solutions of the above described coupled equations. For tractable results, we shall discuss some of the special cases under appropriate assumptions.

C. Special Cases

For the linearized case (or the liquid limit)[39], the absorbed energy of the surface layer is instantly and locally thermalized, i.e., the diffusion term is neglected and the internal energy reaches its steady-state obtained by taking the limit of $D \to 0$ and $\tau \to 0$ in Eq. (29),

$$U_s = \frac{\tau n \alpha c}{4\pi}(E_1 E_3^* + E_2^* E_4) \quad . \tag{38}$$

In this case Eq. (30) becomes a usual heat diffusion equation

$$(\frac{\partial}{\partial t} + \Gamma_T - D\frac{\partial^2}{\partial z^2})T_1 - F_1\dot{\rho}_1 = S \quad , \tag{39}$$

$$S = (\frac{F}{\tau C_V B_T})U_s \, e^{-\alpha z} \quad , \tag{40}$$

where we have generalized the heat diffusion equation into the three-dimensional system where the heat diffusion in the radial direction causes the decay of the thermal grating given by $\Gamma_T = Dq^2$, and heat absorption of the surface layer in the normal (z) direction causes the LIPS via the non-uniform thermal expansion of the surface layer. F_1 is a coupling constant and $\dot{\rho}_1$ denotes for the time derivative of the density. We shall now calculate the amplitude (height) of LIPS based on a simplified version of

Eq. (39) called the "surface heating" system. This reduces the "volume heating" system of Eqs. (39) and (40) into[34]

$$(\frac{\partial}{\partial t} + \Gamma_T)T_1 = D\frac{\partial^2}{\partial z^2} T_1 + F_1\dot{\rho}_1 \quad , \tag{41}$$

with the initial condition $T_1(t = 0) = 0$ and boundary condition

$$K\frac{\partial T_1}{\partial z}\Big|_{z = 0} = -(1 - R)E_0 \quad , \tag{42}$$

where R is the usual reflectivity of the incident $E_{1,2}$ and the reflected $E_{3,4}$ wave, and E_0 is defined by $E_0 \equiv E_1E_3^* + E_2^*E_4$ evaluated on the surface plan, $z = 0$. Under the condition of isotropic thermal expansion, the amplitude of LIPS is given by

$$Q(t) = \frac{B_T}{3}\int_0^\infty dz\ T_1(z,t) \quad . \tag{43}$$

Thus the variation of Q(t) is governed by

$$(\frac{\partial}{\partial t} + \Gamma_T)Q(t) = B_T(1-R)E_0/3 \quad , \tag{44}$$

where we have neglected the density coupling term, and in deriving Eq. (44), we have used Eqs. (41) and (42) and also assumed $(\partial T_1/\partial z)$ at $z = \infty$ is zero. The amplitude (height) of LIPS may then be calculated from Eq. (44) whose exact solution, for $Q(T = 0) = 0$, is given by

$$Q(t) = \frac{(1-R)B_T}{3}\int_0^t dt'\ e^{\Gamma_T(t'-t)}E_0(t') \quad . \tag{45}$$

We note that the time-dependent profile of the LIPS depends upon the thermal grating decay rate, Γ_T, and the evolution of the fields $E_0(t) = E_1(t)E_3^*(t) + E_2^*(t)E_4(t)$ evaluated at the interface plan $z = 0$. For the cw or square pulse case, it is easy to find

$$Q(t) = \frac{(1-R)B_T}{3\Gamma_T}(1 - e^{-\Gamma_T t})E_0 \quad , \tag{46a}$$

$$\Gamma_T = Dq^2 = D(\frac{4\pi n}{\lambda})^2 \sin^2(\frac{\theta}{2}) \quad , \tag{46b}$$

where the steady-state amplitude, for $\Gamma_T t >> 1$, is proportional to E_0/Γ_T. We note that formation of LIPS with significant amplitude requires two conditions: high enough applied field (E_0) and long enough thermal grating lifetime, i.e., small damping factor Γ_T. Because Γ_T is proportional to Dq^2, we require a small diffusion coefficient (D) and a small angle, i.e., $q = 2k\sin(\frac{\theta}{2})$ is small. The latter condition may be achieved by lasers with short wavelength and/or by small propagation angle between the pump ($\vec{E}_1$) and the probe ($\vec{E}_3$) field.

To include the density fluctuation effects in LIPS, the following coupled equations may be obtained

$$\ddot{P} + \Gamma_p \dot{P} + \Omega_0^2 P + F_2 Q = B_1 E_0 \quad , \tag{47}$$

$$\dot{Q} + \Gamma_T Q + F_1 P = B_2 E_0 \quad , \tag{48}$$

wherewhere P is the density fluctuation (or laser-pressure) induced amplitude of LIPS, Γ_p and Ω_0 are the associated damping factor and frequency, and $F_{1,2}$ and $B_{1,2}$ are the appropriate coupling constants. The steady-state solution of Eqs. (47) and (48) is straightforward and will not be shown here. We, however, note that the overall amplitude of LIPS in general is a complex variable and time-dependent.

D. Reflectivity of PCS

The reflectivity of PCS defined by $R_{PCS} = |E_4|^2/|E_3|^2$ evaluated on the $z = 0$ plane, in general, is time-dependent. Again, numerical methods are required for the transient values. For the case of a strong pump, with $E_{1,2}$

>> $E_{3,4}$, the steady-state equations (35) and (36) for the case of $\beta_{1,3} \ll \beta_{2,4}$ and $\beta_2 = \beta_4 = \beta$ yield

$$R_{PCS} = \left|\frac{E_4(0)}{E_3(0)}\right|^2 = \tan^2(|\beta E_1(0)E_2(0)L|) \quad , \tag{49}$$

where β is proportional to the decay time of the thermal grating defined in Eq. (34) and L is the effective thickness of the absorbing layer for the phase-conjugated back scattering to occur. We note that in the low-reflectivity limit and $E_1(0) = E_2(0) = I^{\frac{1}{2}}$, Eq. (49) reduces to Eq. (23) when L = 1. Furthermore, the PCS reflectivity can actually be much higher than one, i.e., the phase-conjugated wave (E_4) is coupled to the strong pump fields (E_1 and E_2) and its intensity is "amplified" to a level much higher than that of the probe field (E_3). The infinite peaks are predicted from Eq. (49) when the conditions of $\tan x = (n + \frac{1}{2})\pi$ are met.[11] We should, however, note that this behavior occurs only at the weak signal limit and does not occur when the pump depletion is included (strong signal case).

5. Applications and Summary

In this paper we have reviewed the resonance fluorescence of two-level atoms on both smooth and rough surfaces. For a system of smooth surface, we have shown the oscillatory behavior for both the resonance fluorescence and the adatom lifetime as a function of the adatom-surface distance (referred to Fig. 1). For an adatom on a rough surface, we found that the sharp resonance enhancement caused by the plasmons excitation occurs for a specific shape of the prolate hemispheroid (see Fig. 2). Results obtained from this system can provide us useful characterization in the area of surface chemistry, such as the orientation and structure of the adspecies, the strength of the adatom-surface coupling and the role of surface roughness on the lifetime and fluorescence of the adspecies.

For phase-conjugated systems, we have proposed a new phenomenon in Section 3, of dipole radiation on a PCS where the dipole lifetime can actually be infinite. In a pumping process, the reflected field may be "amplified" by a set of counter-propagating strong fields. In Section 4, we have discussed LIPS caused by the interference between two incident waves. The phase-conjugated field, originated from the optical nonlinear effects of the absorbing layer, may be achieved with a reflectivity much larger than one. Applications of LIPS include, for example, (i) formation of microstructures for microelectronic fabrication, where the spacing between the periodic gratings is only limited by the laser wavelength and the incident angles of the beams [Eq. (46b)]; (ii) for the application of real time holography, greater resolving power is necessary, i.e., greater PCS reflectivity operated at a larger angle (θ). This may be achieved by higher incident beam intensities and/or shorter wavelengths. The materials suitable for the above described applications will be an absorbing dye with very high absorptibility and very low thermal conductivity but high bulk expansion coefficient, referred to Eq. (45). An experimental study of LIPS using a He-Ne laser and an absorbing layer of epoxy resin mixing with a brilliant, green dye has been reported.[40]

Acknowledgments

This research was supported by the Air Force Office of Scientific Research (AFSC), United States Air Force, under Contract F49620-86-C-0009, and the Office of Naval Research. The United States Government is authorized to reproduce and distribute reprints for governmental purposes, notwithstanding any copyright notation hereon.

REFERENCES

1. T. J. Chuang, Surf. Sci. Rep. 3, 1 (1983).

2. D. J. Ehrlich and J. Y. Tsao, J. Vac. Sci. Tech. B 1, 969 (1983).

3. J. T. Lin, W. C. Murphy and T. F. George, Ind. Eng. Chem. Prod. Res. Dev. 23, 334 (1984).

4. J. T. Lin, M. Hutchinson and T. F. George, in Advances in Multiphoton Processes and Spectroscopy, ed. by S. H. Lin, (World Scientific, Singapore, 1984), pp. 105-237.

5. T. F. George, J. T. Lin, A. C. Beri and W. C. Murphy, Prog. Surf. Sci. 16, 139 (1984).

6. T. F. George, J. T. Lin, K. S. Lim and C. Chang, Opt. Eng. 19, 100 (1980).

7. X. Y. Huang, J. T. Lin and T. F. George, J. Chem. Phys. 80, 893 (1984).

8. X. Y. Huang and T. F. George, J. Phys. Chem. 88, 4801 (1984).

9. X. Y. Huang, K. T. Lee and T. F. George, J. Chem. Phys. 85, 567 (1986).

10. D. Agassi and T. F. George, Surf. Sci. 172, 230 (1986).

11. R. A. Fisher, Ed., Optical Phase Conjugation, (Academic Press, New York 1983).

12. B. Ya. Zeldovich; N. F. Pilipetsky and V. V. Shkunov, Principle of Phase Conjugation (Springer-Verlag, New York 1985).

13. See the review by R. R. Chance, A. Prock and R. Silbey, Adv. Chem. Phys. 37, 1 (1978).

14. M. R. Philpott, Chem. Phys. Lett. 19, 435 (1973).

15. H. Morawitz, Phys. Rev. 187, 1792 (1969).

16. R. R. Chance, A. Prock and R. Silbey, J. Chem. Phys. 60, 2744 (1974).

17. K. H. Drexhage, J. Lumin. 1/2, 693 (1970).

18. H. Kuhn, J. Chem. Phys. 53, 101 (1970)

19. X. Y. Huang, K. C. Liu and T. F. George, in Laser-Controlled Chemical Processing of Surfaces, ed. by A. W. Johnson, D. J. Ehrlich and H. R. Schlossberg (Elsevier, New York), Mat. Res. Soc. Symp. Proc. 29, 381 (1984).

20. X. Y. Huang, T. F. George and J. Lin, in Coherence and Quantum Optics V, ed. by L. Mandel and E. Wolf (Plenum, New York, 1984), pp. 675-693.

21. J. Lin, X. Y. Huang and T. F. George, Solid State Commun. 47, 63 (1983).

22. J. Gersten and A. Nitzan, J. Chem. Phys. 73, 3023 (1980).

23. A. C. Pineda and D. Ronis, J. Chem. Phys. 83, 5330 (1985).

24. H. Metiu, Prog. Surf. Sci. 17, 153 (1984).

25. B. R. Mollow, Phys. Rev. 188, 1969 (1969).

26. X. Y. Huang and T. F. George, manuscript in preparation.

27. H. Kuhn, J. Chem. Phys. 53, 101 (1970).

28. A. Sommerfeld, Ann. Phys. Leipz. 28, 665 (1909); A. Sommerfeld, Ann. Phys. Leipz. 81, 1135 (1926).

29. A. A. Maradudin, in Surface Polaritons, ed. by V. M. Agraovich and D. L. Mills (North-Holland, Amsterdam, 1982), pp. 405-510.

30. P. M. Fauchet and A. E. Siegman, Appl. Phys. Lett. 40, 1678 (1982).

31. S. R. Brueck and D. J. Ehrlich, Phys. Rev. Lett. 48, 1678 (1982).

32. G. N. Marcas, G. L. Harris, C. A. Lee and R. A. McFarlane, Appl. Phys. Lett. 33, 453 (1978).

33. B. Ya. Zeldovich, N. F. Pilipetsky, A. N. Sudarkin and V. V. Shkunov, Sov. Phys. Dokl. 25, 377 (1980).

34. J. T. Lin and T. F. George, J. Appl. Phys. 54, 382 (1983).

35. W. Lee and C. C. Davis, IEEE J. Quantum Electron. QE-22, 569 (1986).

36. N. M. Lawandy, IEEE J. Quantum Electron. QE-19, 1359 (1983).

37. I. L. Fabelinski, in Quantum Electronics: A Treatise, Vol I, ed. by H. Rabin and C. L. Tang (Academic Press, New York 1975), pp. 364-418.

38. I. P. Batra, R. H. Enns and D. Bohl, Phys. Status Solidi 48, 11 (1971).

39. R. M. Herman and M. A. Gray, Phys. Rev. Lett. 19, 824 (1967).

40. R. J. Lysiak, private communication.

Figure Captions

1. Atom-surface distance dependence of the heights of the three peaks in the resonance fluorescence spectrum for the case of a silver surface, where H_-, H_0 and H_+ correspond to the peak heights (in arbitrary units) of the three-photon, incoherent Rayleigh and fluorescence components, respectively. D = 2kd is the reduced distance, where k is the wavenumber and d is the atom-surface distance. The Drude model is used for the dielectric function of the metal, while the dielectric function of the gas medium is set equal to one. The detuning $\omega_{21} - \omega_L$ is 1 A and the Rabi frequency is 10 A, in the unit of Einstein's A-coefficient for spontaneous decay. The solid curves are for the induced transition dipole of the atom oriented perpendicular to the surface, and the dashed curves are for the parallel case.
2. Rough surface-induced phase-decay constant γ_s as a function of the semi-minor axis b of the surface protrusion, where the semi-major axis is fixed at 100 Å. γ_s is in the unit of Einstein's A-coefficient.
3. Geometry of an electric dipole in a phase-conjugated (time-reversal) cavity. The dipole with moment $\vec{\mu} = \mu\vec{e}_3$ is located at the center of the cavity, where $\vec{e}_3$ is the unit vector along the x_3-axis. The emitted radiation field at the point (r,θ) is denoted by (E_r, E_θ) inside the cavity.
4. Normalized decay rate constant $\bar{b}$ of the dipole versus η_2/η_1, with fixed reflectivity $|\eta|$: (a) $|\eta| = 1\%$; (b) $|\eta| = 2\%$ (c) $|\eta| = 3\%$. The results show that the lifetime of the dipole is sensitive to $|\eta|$ and η_2/η_1 of the PCM cavity. There is a critical value of η_2/η_1 that leads to $\bar{b} \simeq 0$, i.e., the lifetime approaches infinity. In these curves, the values of $\lambda = 0.3$ μm and $r_0 = 100$ Å are used.

5. Schematic diagram of laser-induced periodic structure, where E_1 and E_3 are the incident waves with a phase mismatching vector $\Delta\vec{k}$. The amplitude and lifetime of the intereference pattern are governed by $|\Delta\vec{k}|^2$.

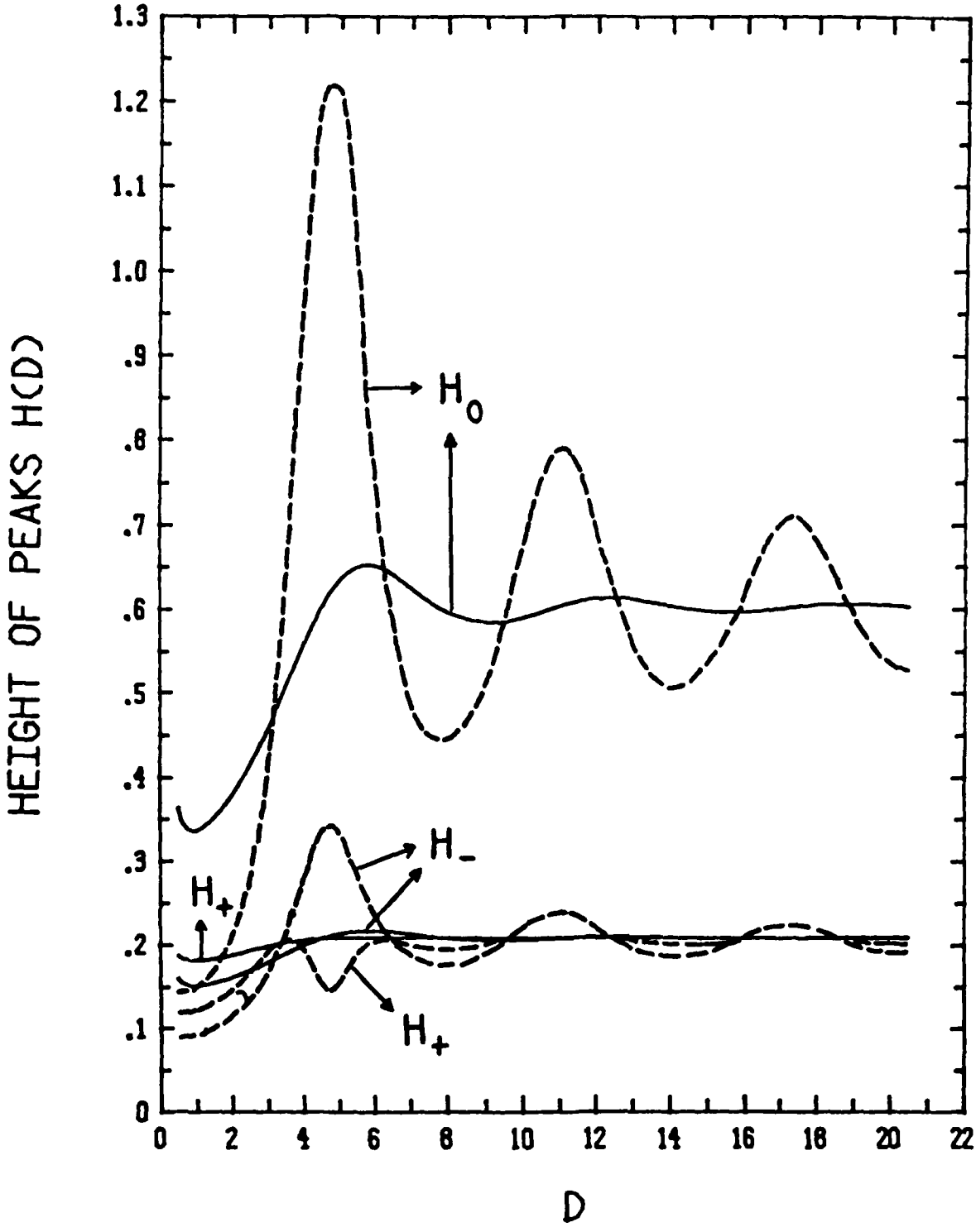
HEIGHT OF PEAKS H(D)
1.3
1.2
1.1
1.0
.9
.8
.7
.6
.5
.4
.3
.2
.1
0
0
2
4
6
8
10
12
14
16
18
20
22
D
H_0
H_-
H_+
H_+

Fig. 1

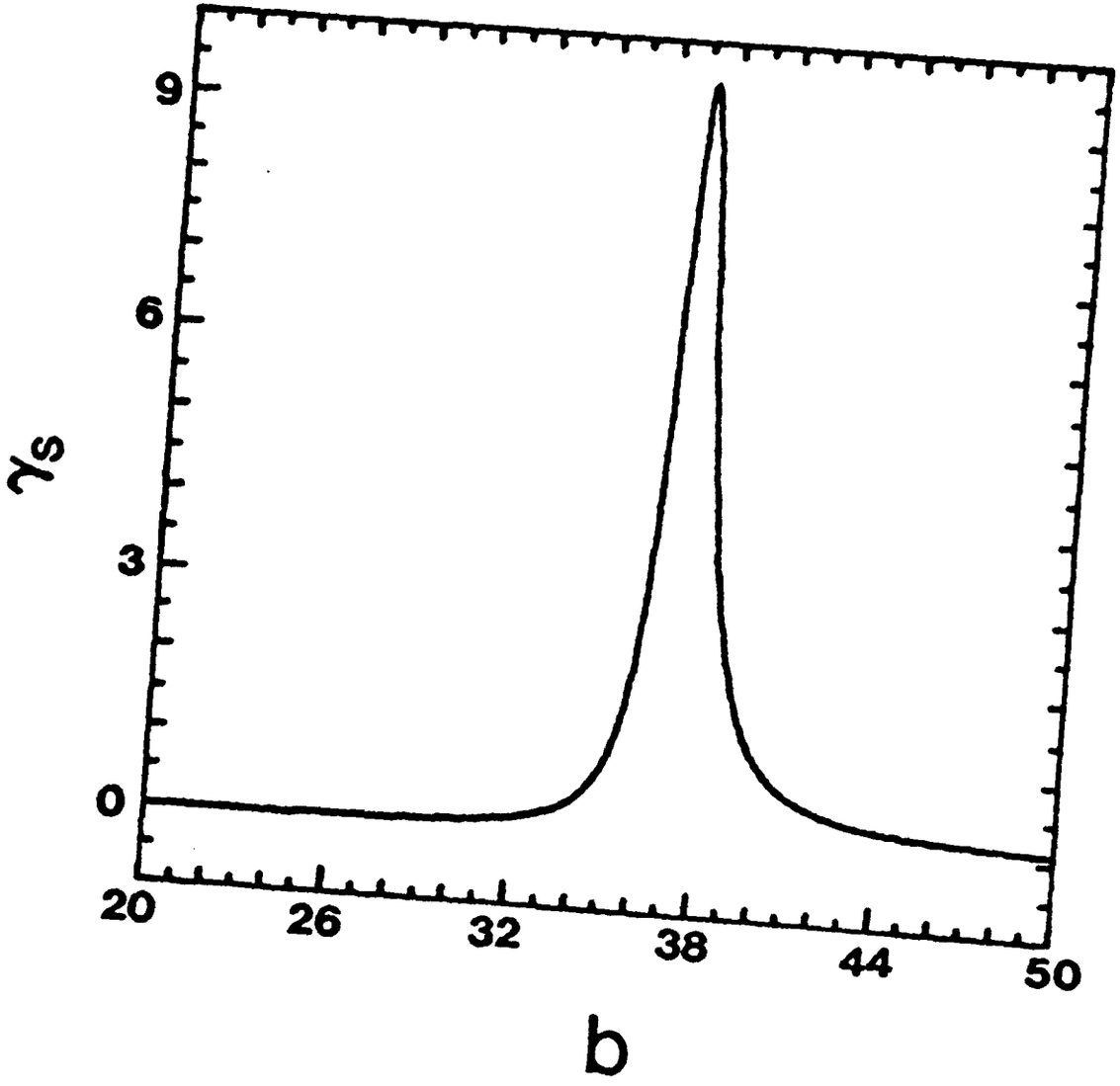

Fig. 2

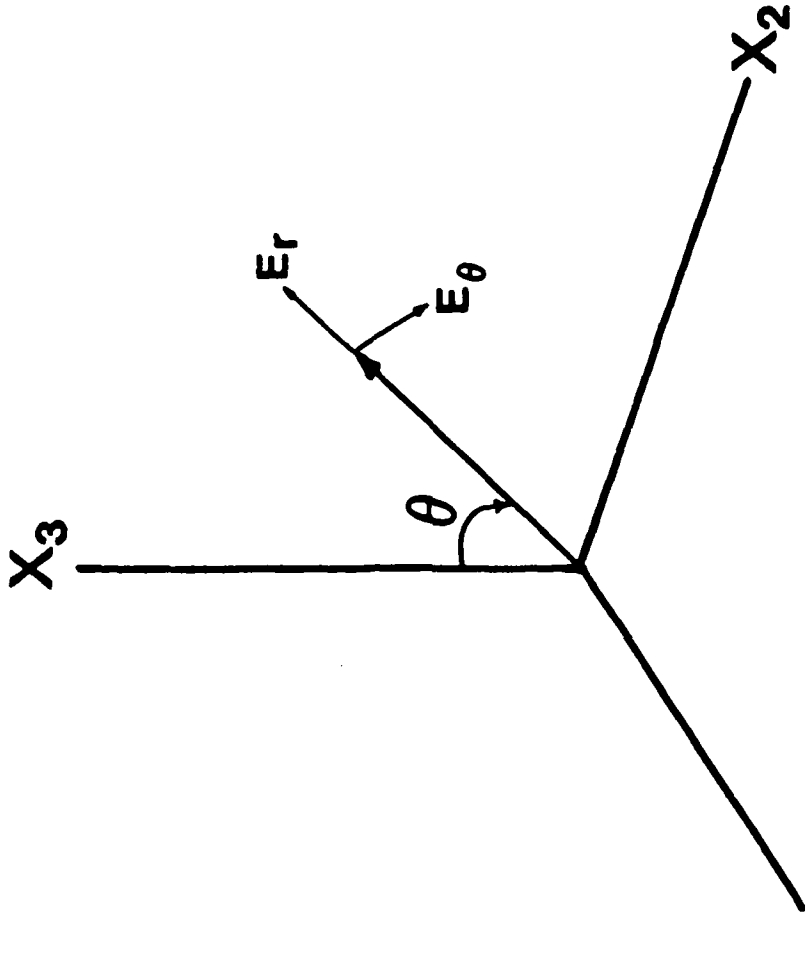

Fig. 3

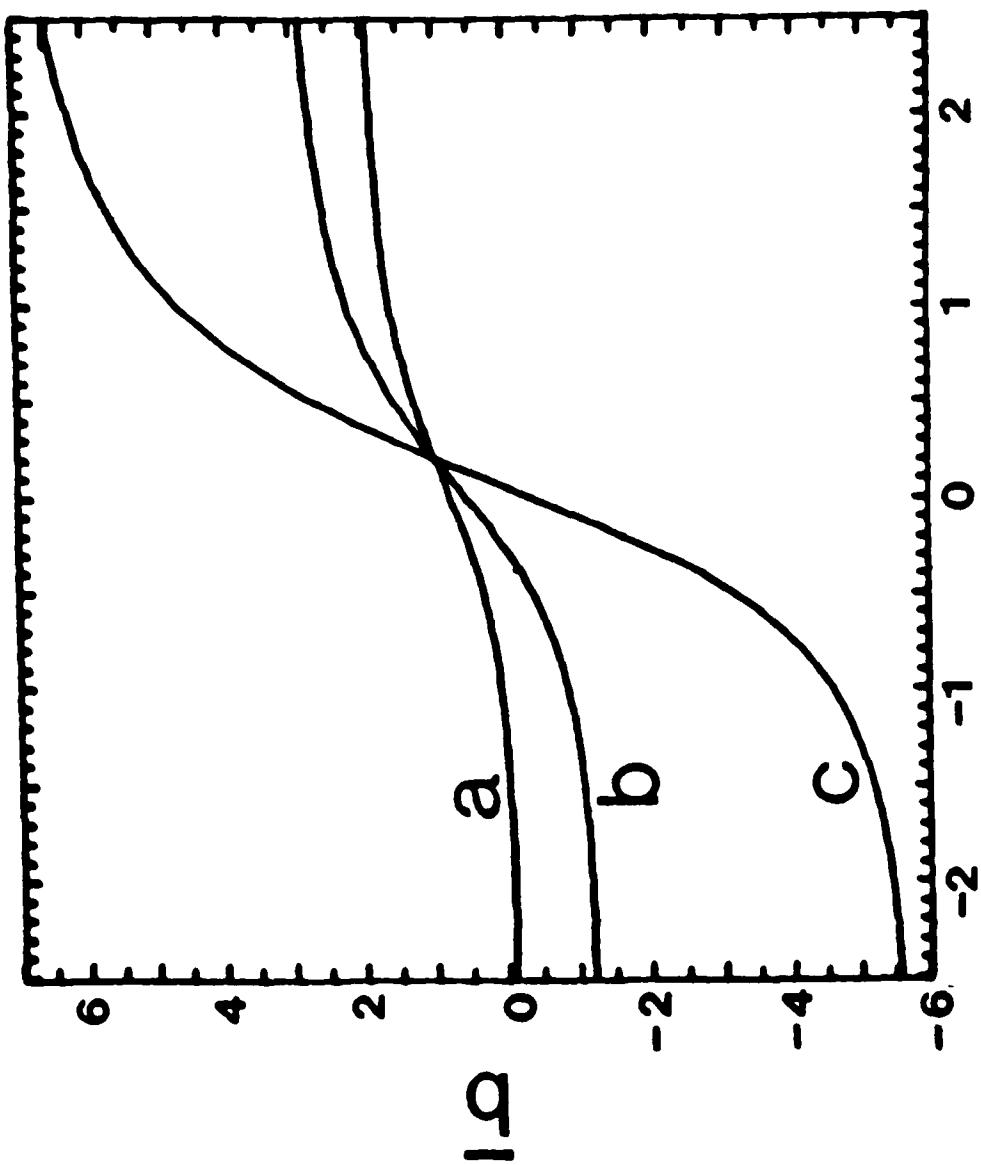

Fig. 4

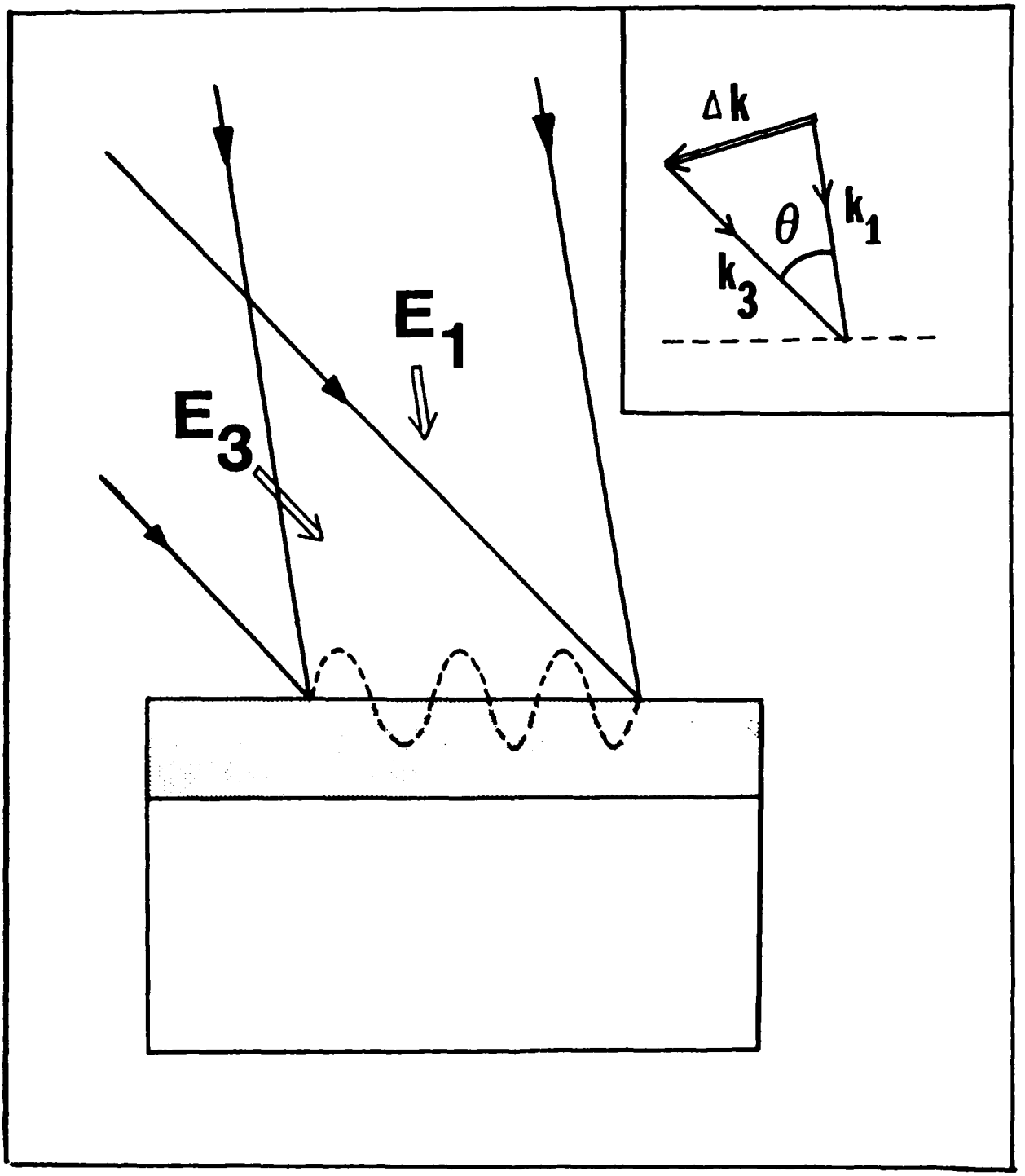

Fig. 5

TECHNICAL REPORT DISTRIBUTION LIST, GEN

	No. Copies
Office of Naval Research Attn: Code 1113 800 N. Quincy Street Arlington, Virginia 22217-5000	2
Dr. Bernard Douda Naval Weapons Support Center Code 50C Crane, Indiana 47522-5050	1
Naval Civil Engineering Laboratory Attn: Dr. R. W. Drisko, Code L52 Port Hueneme, California 93401	1
Defense Technical Information Center Building 5, Cameron Station Alexandria, Virginia 22314	12 high quality
DTNSRDC Attn: Dr. H. Singerman Applied Chemistry Division Annapolis, Maryland 21401	1
Dr. William Tolles Superintendent Chemistry Division, Code 6100 Naval Research Laboratory Washington, D.C. 20375-5000	1
Dr. David Young Code 334 NORDA NSTL, Mississippi 39529	1
Naval Weapons Center Attn: Dr. Ron Atkins Chemistry Division China Lake, California 93555	1
Scientific Advisor Commandant of the Marine Corps Code RD-1 Washington, D.C. 20380	1
U.S. Army Research Office Attn: CRD-AA-IP P.O. Box 12211 Research Triangle Park, NC 27709	1
Mr. John Boyle Materials Branch Naval Ship Engineering Center Philadelphia, Pennsylvania 19112	1
Naval Ocean Systems Center Attn: Dr. S. Yamamoto Marine Sciences Division San Diego, California 91232	1
Dr. David L. Nelson Chemistry Division Office of Naval Research 800 North Quincy Street Arlington, Virginia 22217	1

ABSTRACTS DISTRIBUTION LIST, 056/625/629

Dr. J. E. Jensen
Hughes Research Laboratory
3011 Malibu Canyon Road
Malibu, California 90265

Dr. J. H. Weaver
Department of Chemical Engineering
and Materials Science
University of Minnesota
Minneapolis, Minnesota 55455

Dr. A. Reisman
Microelectronics Center of North Carolina
Research Triangle Park, North Carolina
27709

Dr. M. Grunze
Laboratory for Surface Science and
Technology
University of Maine
Orono, Maine 04469

Dr. J. Butler
Naval Research Laboratory
Code 6115
Washington D.C. 20375-5000

Dr. L. Interante
Chemistry Department
Rensselaer Polytechnic Institute
Troy, New York 12181

Dr. Irvin Heard
Chemistry and Physics Department
Lincoln University
Lincoln University, Pennsylvania 19352

Dr. K.J. Klaubunde
Department of Chemistry
Kansas State University
Manhattan, Kansas 66506

Dr. C. B. Harris
Department of Chemistry
University of California
Berkeley, California 94720

Dr. F. Kutzler
Department of Chemistry
Box 5055
Tennessee Technological University
Cookesville, Tennessee 38501

Dr. D. DiLella
Chemistry Department
George Washington University
Washington D.C. 20052

Dr. R. Reeves
Chemistry Department
Renssaeler Polytechnic Institute
Troy, New York 12181

Dr. Steven M. George
Stanford University
Department of Chemistry
Stanford, CA 94305

Dr. Mark Johnson
Yale University
Department of Chemistry
New Haven, CT 06511-8118

Dr. W. Knauer
Hughes Research Laboratory
3011 Malibu Canyon Road
Malibu, California 90265

ABSTRACTS DISTRIBUTION LIST, 056/625/629

Dr. G. A. Somorjai
Department of Chemistry
University of California
Berkeley, California 94720

Dr. J. Murday
Naval Research Laboratory
Code 6170
Washington, D.C. 20375-5000

Dr. J. B. Hudson
Materials Division
Rensselaer Polytechnic Institute
Troy, New York 12181

Dr. Theodore E. Madey
Surface Chemistry Section
Department of Commerce
National Bureau of Standards
Washington, D.C. 20234

Dr. J. E. Demuth
IBM Corporation
Thomas J. Watson Research Center
P.O. Box 218
Yorktown Heights, New York 10598

Dr. M. G. Lagally
Department of Metallurgical
and Mining Engineering
University of Wisconsin
Madison, Wisconsin 53706

Dr. R. P. Van Duyne
Chemistry Department
Northwestern University
Evanston, Illinois 60637

Dr. J. M. White
Department of Chemistry
University of Texas
Austin, Texas 78712

Dr. D. E. Harrison
Department of Physics
Naval Postgraduate School
Monterey, California 93940

Dr. R. L. Park
Director, Center of Materials
Research
University of Maryland
College Park, Maryland 20742

Dr. W. T. Peria
Electrical Engineering Department
University of Minnesota
Minneapolis, Minnesota 55455

Dr. Keith H. Johnson
Department of Metallurgy and
Materials Science
Massachusetts Institute of Technology
Cambridge, Massachusetts 02139

Dr. S. Sibener
Department of Chemistry
James Franck Institute
5640 Ellis Avenue
Chicago, Illinois 60637

Dr. Arnold Green
Quantum Surface Dynamics Branch
Code 3817
Naval Weapons Center
China Lake, California 93555

Dr. A. Wold
Department of Chemistry
Brown University
Providence, Rhode Island 02912

Dr. S. L. Bernasek
Department of Chemistry
Princeton University
Princeton, New Jersey 08544

Dr. W. Kohn
Department of Physics
University of California, San Diego
La Jolla, California 92037

ABSTRACTS DISTRIBUTION LIST, 056/625/629

Dr. F. Carter
Code 6170
Naval Research Laboratory
Washington, D.C. 20375-5000

Dr. Richard Colton
Code 6170
Naval Research Laboratory
Washington, D.C. 20375-5000

Dr. Dan Pierce
National Bureau of Standards
Optical Physics Division
Washington, D.C. 20234

Dr. R. Stanley Williams
Department of Chemistry
University of California
Los Angeles, California 90024

Dr. R. P. Messmer
Materials Characterization Lab.
General Electric Company
Schenectady, New York 22217

Dr. Robert Gomer
Department of Chemistry
James Franck Institute
5640 Ellis Avenue
Chicago, Illinois 60637

Dr. Ronald Lee
R301
Naval Surface Weapons Center
White Oak
Silver Spring, Maryland 20910

Dr. Paul Schoen
Code 6190
Naval Research Laboratory
Washington, D.C. 20375-5000

Dr. John T. Yates
Department of Chemistry
University of Pittsburgh
Pittsburgh, Pennsylvania 15260

Dr. Richard Greene
Code 5230
Naval Research Laboratory
Washington, D.C. 20375-5000

Dr. L. Kesmodel
Department of Physics
Indiana University
Bloomington, Indiana 47403

Dr. K. C. Janda
University of Pittsburg
Chemistry Building
Pittsburg, PA 15260

Dr. E. A. Irene
Department of Chemistry
University of North Carolina
Chapel Hill, North Carolina 27514

Dr. Adam Heller
Bell Laboratories
Murray Hill, New Jersey 07974

Dr. Martin Fleischmann
Department of Chemistry
University of Southampton
Southampton 509 5NH
UNITED KINGDOM

Dr. H. Tachikawa
Chemistry Department
Jackson State University
Jackson, Mississippi 39217

Dr. John W. Wilkins
Cornell University
Laboratory of Atomic and
Solid State Physics
Ithaca, New York 14853

ABSTRACTS DISTRIBUTION LIST, 056/625/629

Dr. R. G. Wallis
Department of Physics
University of California
Irvine, California 92664

Dr. D. Ramaker
Chemistry Department
George Washington University
Washington, D.C. 20052

Dr. J. C. Hemminger
Chemistry Department
University of California
Irvine, California 92717

Dr. T. F. George
Chemistry Department
University of Rochester
Rochester, New York 14627

Dr. G. Rubloff
IBM
Thomas J. Watson Research Center
P.O. Box 218
Yorktown Heights, New York 10598

Dr. Horia Metiu
Chemistry Department
University of California
Santa Barbara, California 93106

Dr. W. Goddard
Department of Chemistry and Chemical
Engineering
California Institute of Technology
Pasadena, California 91125

Dr. P. Hansma
Department of Physics
University of California
Santa Barbara, California 93106

Dr. J. Baldeschwieler
Department of Chemistry and
Chemical Engineering
California Institute of Technology
Pasadena, California 91125

Dr. J. T. Keiser
Department of Chemistry
University of Richmond
Richmond, Virginia 23173

Dr. R. W. Plummer
Department of Physics
University of Pennsylvania
Philadelphia, Pennsylvania 19104

Dr. E. Yeager
Department of Chemistry
Case Western Reserve University
Cleveland, Ohio 41106

Dr. N. Winograd
Department of Chemistry
Pennsylvania State University
University Park, Pennsylvania 16802

Dr. Roald Hoffmann
Department of Chemistry
Cornell University
Ithaca, New York 14853

Dr. A. Steckl
Department of Electrical and
Systems Engineering
Rensselaer Polytechnic Institute
Troy, NewYork 12181

Dr. G.H. Morrison
Department of Chemistry
Cornell University
Ithaca, New York 14853

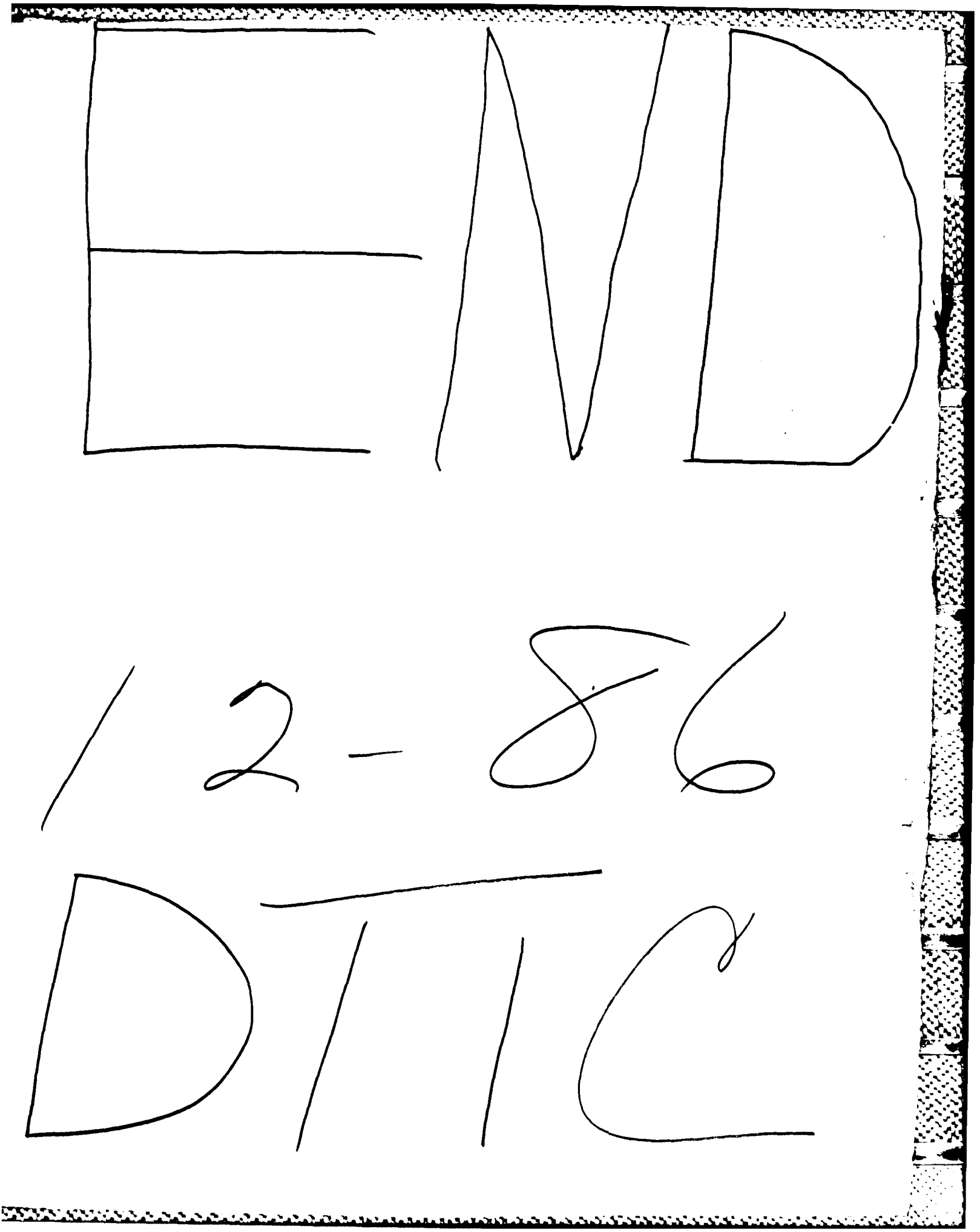
END
12-86
DTIC